PHYSICS POTENTIAL OF VERY INTENSE CONVENTIONAL NEUTRINO BEAMS

JUAN JOSÉ GÓMEZ CADENAS

Instituto de Física Corpuscular, IFIC
Edificio de Institutos de Paterna, 46071 Valencia, Spain
and CERN
Ch-1211 Geneve 23, Switzerland
E-mail: gomez@mail.cern.ch, gomez@ific.uv.es

as a rapporteur from the CERN working group on Super Beams

A. BLONDEL[1], J. BURGUET-CASTELL[2], D. CASPER[3], M. DONEGA[1], S. GILARDONI[1], P. HERNÁNDEZ[4] and M. MEZZETTO[5]

(1) Département de Physique, Université de Geneve, Switzerland
(2) IFIC, Edificio de Institutos de Paterna, Paterna, Valencia, Spain
(3) University of California at Irvine, USA
(4) INFN, sezione di Padova, Italy
(5) CERN, Ch-1211 Geneve 23, Switzerland

ABSTRACT

The physics potential of high intensity conventional beams is explored. We consider a low energy super beam which could be produced by a proposed new accelerator at CERN, the Super Proton Linac. Water Cherenkov and liquid oil scintillator detectors are studied as possible candidates for a neutrino oscillation experiment which could improve our current knowledge of the atmospheric parameters δm^2_{atm},θ_{23} and measure or severely constrain the parameter connecting the atmospheric and solar realms, θ_{13}. It is also shown that a very large water detector could eventually observe leptonic CP violation. The reach of such an experiment to the neutrino mixing parameters would lie in-between the next generation of neutrino experiments (MINOS, OPERA, etc) and a future neutrino factory.

1. Introduction

The notion of "super beams" was introduced by B. Richter, who suggested[1)] that a conventional neutrino beam of very high intensity could be competitive with the pure two-flavor beams produced by the neutrino factory. Recent work[2,3)] has considered in great detail the potential of generic super beams, with neutrino energies ranging from 1 to 50 GeV and baselines spanning from 200 to 7000 kilometers. A large variety of detector technologies, including a liquid argon TPC, a fine grain iron calorimeter and water Cherenkov detectors á la Super-Kamiokande have been discussed as potential candidates for a super beam experiment. The general conclusion reached in[2,3)] is that super beams can largely improve in our knowledge of δm^2_{atm},θ_{23} and θ_{13}, as well as providing some sensitivity to a CP violating phase δ, if the solution of the solar neutrino problem lies in the upper region of the Large Mixing Angle (LMA-MSW). On

the other hand, it is also concluded that ultimate sensitivity to the above parameters, in particular to δ, will require the pure and intense beams of a neutrino factory.

In this paper we present a complementary approach to the work referred above. We consider only a super beam of very low neutrino energy, 250 MeV on average, which was not studied in[2,3]. Such a beam will be produced by the very intense Super Proton Linac[4], a future facility planned at CERN. Furthermore, we restrict ourselves to those technologies which afford truly massive targets (a must, given the low energy of our neutrinos), and therefore consider only water Cherenkov and liquid scintillating oil detectors. In order to estimate the experimental response (e.g., signal efficiency as well as beam and detector-induced backgrounds) we have performed for the water Cherenkov detector a full simulation followed by a detailed analysis using the Super-Kamiokande tools, in contrast with the simple estimations made in[2,3] and, indeed,with our own educated guesses for the liquid scintillating oil detector.

This paper is organized as follows. In section 2 we briefly address the general features of super beams. In section 3 the Super Proton Linac (SPL hereafter) and the resulting, low-energy neutrino beam are described. In section 4 we discuss our detector scenarios. An estimation of the sensitivity to the atmospheric parameters δm^2_{atm},θ_{23}, as well as to θ_{13} and the CP violating phase δ is presented in section 5. In section 6 we conclude.

2. Conventional super beams

A conventional neutrino beam is produced by hitting a nuclear target with an intense hadron beam, then sign-selecting and letting decay the resulting hadrons through a beam decay tunnel. At the end of the tunnel there is an absorber, where the copiously produced muons (a by product of pion and kaon decay) are ranged out before most of them can decay.

The resulting neutrino beam is mostly made of ν_μ(assuming that π^+ were selected). Nevertheless, kaon and muon decays result in small but sizeable contaminations of ν_e and $\overline{\nu}_e$. Opposite sign pion feed-through yields also some contamination of $\overline{\nu}_\mu$. As an example, Figure 1 shows the neutrino beam spectra produced by the 450 GeV Super Proton Syncroton, at CERN, which illuminated the NOMAD[5] and CHORUS[6] experiments.

Notice that the contamination of other neutrino species is a handicap for the so-called neutrino oscillation *appearance* experiments, in which one searches for a flavor not originally in the beam. It has been stressed[7]that the best way of measuring θ_{13} and δ is through the transitions $\nu_\mu \rightarrow \nu_e$. Any contamination of ν_e in the original beam must be subtracted, resulting in loss of sensitivity.

Indeed, this is the key advantage of the neutrino factory beams, produced by the decay of muons circulating in an storage ring, over conventional beams. As shown in Figure 2, the decay of (say) positive muons result in a beam of *pure* ν_e and $\overline{\nu}_\mu$, thus,

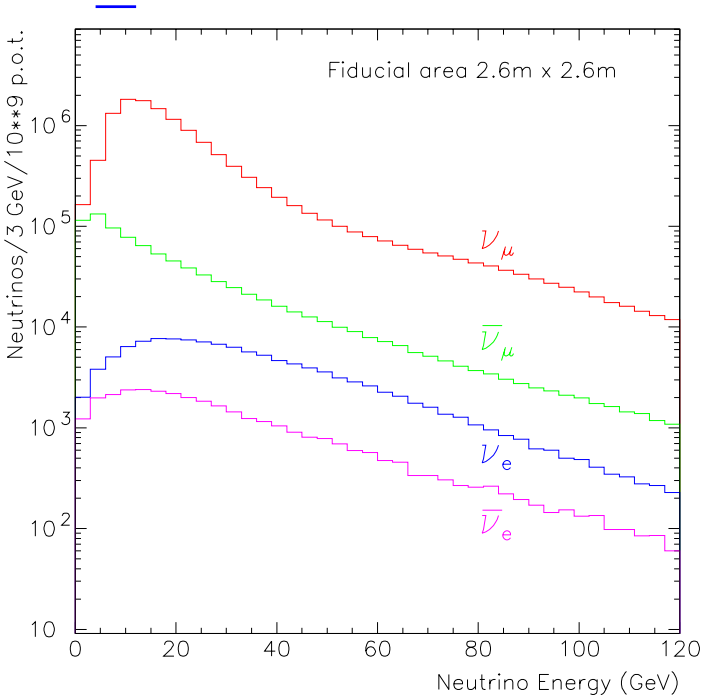

Figure 1: Fluxes produced by the SPS neutrino beam of the CERN West area. Notice that the beam is mostly made of ν_μ but there are contaminations of all other neutrino species, except ν_τ.

there is no beam contamination (assuming, of course, that one is able to measure the charge of the produced lepton) to transitions of the type $\nu_e \to \nu_\mu$.

A super beam is nothing but a conventional beam of stupendous intensity. Thus,(for π^+ selected in the horn), its basic composition is ν_μ with small admixtures of ν_e, $\overline{\nu}_e$ and $\overline{\nu}_\mu$. To gain some appreciation of the relative sensitivity of a conventional neutrino beam and a neutrino factory beam, it is useful to estimate the sensitivity to a $\nu_\mu \to \nu_e$ oscillation search in the appearance mode, *assuming a perfect detector*. Let us assume that the product of the neutrino beam intensity, running time, cross section and detector mass results in a total of N_{μ^-} ν_μ visible interactions, registered by the apparatus, for both the conventional and neutrino factory beams. In addition, in the case of conventional beams, there will be N_{e^-} ν_e visible interactions, due to the intrinsic ν_e contamination, absent in the muon-induced beam. If one is looking for $\nu_\mu \to \nu_e$ oscillations, then, in the neutrino factory[a], the sensitivity goes as:

$$P(\nu_\mu \to \nu_e) \propto \frac{1}{N_\mu} \tag{1}$$

[a]in reality at the neutrino factory one measures the transitions $\nu_e \to \nu_\mu$, since in a massive detector one can measure much more easily the charge of muons than the charge of electrons

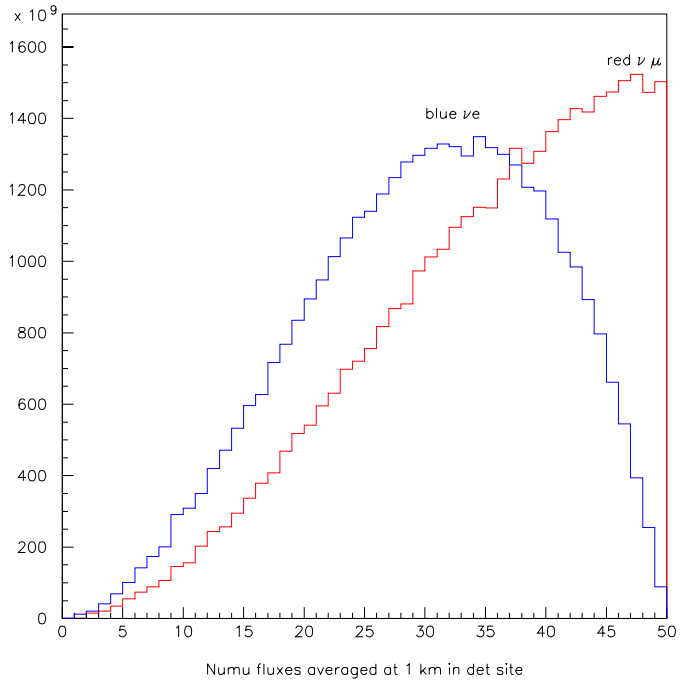

Figure 2: Neutrino beams produced by positive muon decay in an accumulator ring. Notice that this is a pure two-flavor beam, which no contamination of other neutrino species.

since there is no ν_e contamination, while, in the case of a conventional beam, one has:

$$P(\nu_\mu \rightarrow \nu_e) \propto \frac{\sqrt{N_e}}{N_\mu} \tag{2}$$

so, that if the ν_e contamination is a fraction f of the primary ν_μ beam (assuming for simplicity identical ν_e and ν_μ cross sections) we have:

$$P(\nu_\mu \rightarrow \nu_e) \propto \frac{g}{\sqrt{N_\mu}} \tag{3}$$

where $g = \sqrt{f}$. Although g is a small quantity, the key difference between conventional and muon-induced beams is clear comparing equations 1 and 3. In the first case the sensitivity improves *linearly* while in the second improves only with the square root of the total collected statistics.

Another issue concerns systematics in beam composition. While the neutrino spectra from muon decay can be computed to a great precision, the convoluted spectra in a conventional beam are affected by a number of uncertainties, the most important of which is the initial π/K ratio in the hadron beam, which affects the composition of the ν_μ:ν_e:$\overline{\nu}_\mu$:$\overline{\nu}_e$ beam. Typically, these and other uncertainties translate into a

systematic error at the level of few per cent in the conventional neutrino fluxes, to be compared with a few per mil, in the case of a neutrino factory.

Other important aspects to be considered when designing a conventional beam are whether one prefers a wide or narrow band beam and the energy regime. Beam energies range typically from few hundred MeV to few hundred GeV, depending of the colliding hadron beam and beam optics. High energy yields more interactions, sufficiently low energy, we argue, a better control over backgrounds and less beam uncertainties. We refer again to[2,3] for comparison of various energy regimes.

3. The SPL neutrino beam

Mean beam power	4MW
Kinetic energy	2.2 GeV
Repetition rate	75Hz
Pulse duration	2.2 ms
Number of protons per pulse (per second)	$1.5\ 10^{14}(1.1\ 10^{16})$
Mean current during a pulse	11 mA
Overall lenght	799 m
Bunch frequency (minimum time between bunches)	352.2 MHz (2.84 ns)

Table 1: Basic SPL characteristics.

The planned Super Proton Linac is a proton beam of 4 MW power which will be used as a first stage of the Neutrino Factory complex. Its basic parameters are reported in Table 1. Pions are produced by the interactions of the 2.2 GeV proton beam with a liquid mercury target and focused (or defocused, depending on the sign) with a magnetic horn (see Figure 3). Next they transverse a cylindrical decay tunnel of 1 meter radius and 20 meters length (found to be the optimal decay length in[8]). We have used the `MARS` program[9] to generate and track pions, then analytical calculations, described in[8] to compute the probability that the neutrinos produced in both muon and pion decay reach a detector of transverse dimensions A located at a distance L from the target.

The resulting neutrino spectra is shown in Figure 4. Notice that the average energy of the neutrinos is around 250 MeV and that the ν_e contamination of the beam is at the level of few per mil. Due to the low energy of protons, kaon production is strongly suppressed, resulting in both less ν_e contamination and better controlled beam systematics.

4. Detector scenarios

Figure 5 shows the oscillation probability $P(\nu_\mu \rightarrow \nu_e)$as a function of the distance (for $\delta m_{23} = 3 \cdot 10^{-3}$ eV^2 θ_{23}= 45°). Notice that the first maximum of the oscillation is

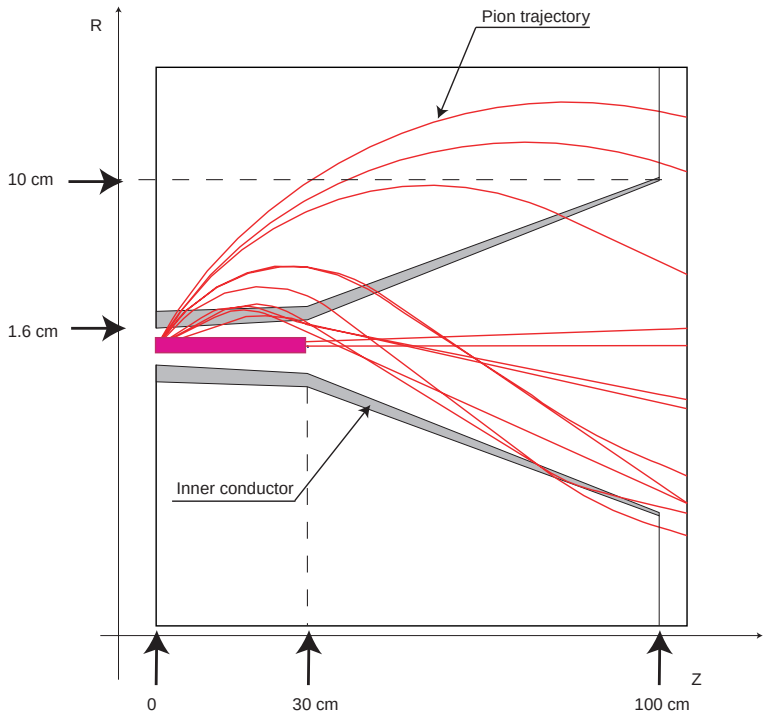

Figure 3: The horn focusing system.

at 100 km. Detection of low-energy neutrinos at O(100 km) from the source requires a massive target with high efficiency. Moreover, a search for ν_e appearance demands excellent rejection of physics backgrounds, namely μ mis-identification and neutral current π^0 production, which should be controlled to a lower level than the irreducible beam-induced background.

In this paper we consider two detector technologies, which have demonstrated excellent performance in the low energy regime, while being able to provide massive targets. These are, water Cherenkov detectors, which have been developed by experiments such as IMB[10)], Kamiokande[11)], and Super-Kamiokande[12)], and diluted liquid scintillator detectors. This type of detectors were used by the LSND experiment[13)] and are being planned for the forthcoming MiniBoone experiment[14)], where both Cherenkov and scintillation light is measured.

In spite of the fact that liquid scintillator apparatus provide, a priory, more handles to reject backgrounds than their water Cherenkov counterparts, the only truly massive detectors built so far are of the latest type (compare Super-Kamiokande 50 ktons with the sparse 499 tons of MiniBoone). For the water detector we have conducted an extensive simulation followed by a full data analysis. Instead, for the liquid scintillating detector, we have worked out an educated guess, extrapolating published data, mainly from LSND and MiniBoone. It is remarkable, however, the good level of agreement that both approaches yield, as will be shown in the remaining of the

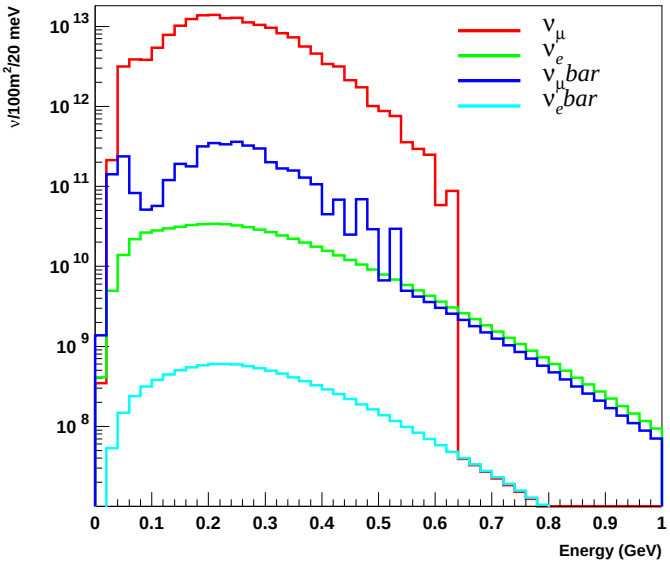

Figure 4: The SPL neutrino spectra, for π^+ focused in the horn. The fluxes are computed at 50 km from the target, then scaled to the relevant distances.

section.

As a base line we have considered 130 km, which is near the maximum of the oscillation and equals the distance between CERN and the Modane laboratory in the FREJUS tunnel, where one could conceivably locate a large neutrino detector[16,18].

4.1. Water Cherenkov detectors

We have considered an apparatus of 40 kton fiducial mass and sensitivity identical to the Super-Kamiokande experiment. The response of the detector to the neutrino beams discussed in section 3 was studied using the NUANCE[17] neutrino physics generator and detector simulation and reconstruction algorithms developed for the Super-Kamiokande atmospheric neutrino analysis. These algorithms, and their agreement with real neutrino data, have been described elsewhere[12,21,20].

In the absence of neutrino oscillations, the dominant reaction induced by the beam is ν_μ quasi-elastic scattering, leading to a single observed (prompt) muon ring. Recoiling protons are well below Cherenkov threshold at the energies discussed here, and hence produce no rings. To unambiguously identify a potentially small ν_e appearance signal, it is essential to avoid confusion of muons with electrons. Thanks to the low energy of the SPL and its neutrino beam, the Cherenkov threshold itself helps separate muons and electrons, since a muon produced near the peak of the spectrum ($\sim 300\,\mathrm{MeV/c}$) cannot be confused with an electron of comparable momentum; instead it will appear to be a much lower-energy ($\sim 100\,\mathrm{MeV/c}$) electron.

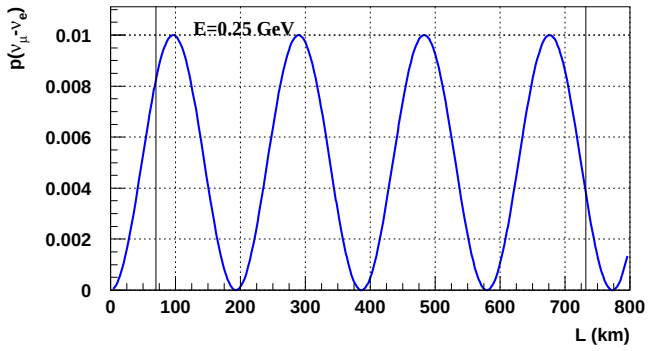

Figure 5: The oscillation probability $P(\nu_\mu \to \nu_e)$, showing a first maximum around 100 km.

Particle identification exploits the difference in the Cherenkov patterns produced by showering ("e-like") and non-showering ("μ-like") particles. Besides, for the energies of interest in this beam, the difference in Cherenkov opening angle between an electron and a muon can also be exploited. Furthermore, muons which stop and decay (100% of μ^+ and 78% of μ^-) produce a detectable delayed electron signature which can be used as an additional handle for background rejection.

For this study, we have used the Super-Kamiokande particle identification criteria, which are based on a maximum likelihood fit of both μ-like and e-like hypotheses. In terms of the particle identification estimator P, shown in Figure 6, an event is e-like if $P_e > P_\mu + 1$. This cut introduces only a small inefficiency for true ν_e charged-current interactions, while reducing the ν_μ background considerably. In addition, any event with an identified muon decay signature is rejected from the e-like (ν_e appearance) sample.

Production of π^0 through neutral current resonance-mediated and coherent processes is another major source of background, which is, however, suppressed by the low energy of the beam and the relatively small boost of the resulting π^0. This results in events where the two rings are easily found by an standard π^0 search algorithm, á la Super-Kamiokande. However, for the events in which only a single ring is found we further apply an algorithm[23], specially tailored to search for low-energy γ's (typically produced by asymmetric decays). The algorithm *always* identifies a candidate for a second ring, which, if the primary ring is truly a single electron, is typically either very low energy, or extremely forward. If, on the other hand, two γ from π^0 decay are present, the second ring-candidate is usually the π^0 daughter which was missed by the standard pattern-recognition. By requiring that the invariant mass formed by the primary ring and the secondary ring-candidate is less than $45\,\mathrm{MeV}/c^2$, almost all remaining π^0 contamination of the single-ring, e-like sample is removed.

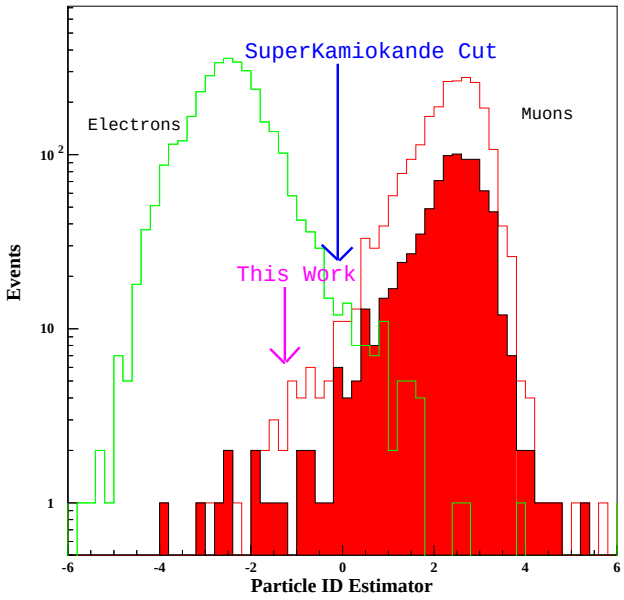

Figure 6: Rejection of ν_μ^{CC} background in a water Cherenkov detector. The particle ID estimator P (in arbitrary units) is shown for the electron-like signal (left) and muon-like background (right). The cut is set at -1, reducing miss-identification of muons considerably at a negligible cost in signal efficiency. Since most ν_μ^{CC} events are followed by a muon-decay signature, the background is further reduced by accepting only events without a delayed coincidence (shaded histogram on right).

The background in each category (ν_μ charged-currents, ν_e contamination in the beam, and neutral currents) remaining after all selections, and the efficiency for signal, after each cut is summarized in Table 2 for the π^+ focused beam and Table 3 for the π^- focused beam. Contamination by ν_e from muon decay in the secondary beam is dominant.

4.2. Liquid scintillator detectors

Liquid scintillator technology has been used by the LSND experiments[13] to detect an small amount of low energy ν_e events in an intense ν_μ beam. The very same technique will be used by the forthcoming MiniBoone experiment[14].

In diluted liquid scintillator detectors both Cherenkov and scintillation lights are measured. They can be separated given the different light emission timing and direction. The Cherenkov light pattern can be used to separate π^0 and μ from electrons

Channel	Initial sample	Visible events	Fit in fiducial volume Single-ring $100-450\,\mathrm{MeV}/c^2$	Tight particle ID	No $\mu \to e$	$m_{\gamma\gamma} < 45\,\mathrm{MeV}/c^2$
ν_μ^{CC}	3250	887	578.4	5.5	2.5	1.5
ν_e^{CC}	18	12.	8.2	8.0	8.0	7.8
NC	2887	36.9	8.7	7.7	7.7	1.7
$\nu_\mu \to \nu_e$		82.4%	77.2%	76.5%	70.7%	

Table 2: Summary of simulated data samples a π^+ focused neutrino beam. The first three lines show the expected background surviving the selection at each stage for a 5-year exposure of a 40 kton (fiducial) water detector located at 130 km from the source. The bottom line shows the efficiencies for the $\nu_\mu \to \nu_e$ signal. The numbers in the rightmost column (after all cuts) represent the sample used to estimate the oscillation sensitivity.

Channel	Initial sample	Visible events	Fit in fiducial volume Single-ring $100-450\,\mathrm{MeV}/c^2$	Tight particle ID	No $\mu \to e$	$m_{\gamma\gamma} < 45\,\mathrm{MeV}/c^2$
$\bar{\nu}_\mu^{CC}$	539	186	123	2.3	0.7	0.7
$\bar{\nu}_e^{CC}$	4	3.3	3	2.7	2.7	2.7
NC	687	11.7	3.3	3	3	0.3
$\bar{\nu}_\mu \to \bar{\nu}_e$		79.3%	74.1%	74.0%	67.1%	

Table 3: Summary of simulated data samples a π^- focused neutrino beam. The first three lines show the expected background surviving the selection at each stage for a 5-year exposure of a 40 kton (fiducial) water detector located at 130 km from the source. The bottom line shows the efficiencies for the $\bar{\nu}_\mu \to \bar{\nu}_e$ signal. The numbers in the rightmost column (after all cuts) represent the sample used to estimate the oscillation sensitivity.

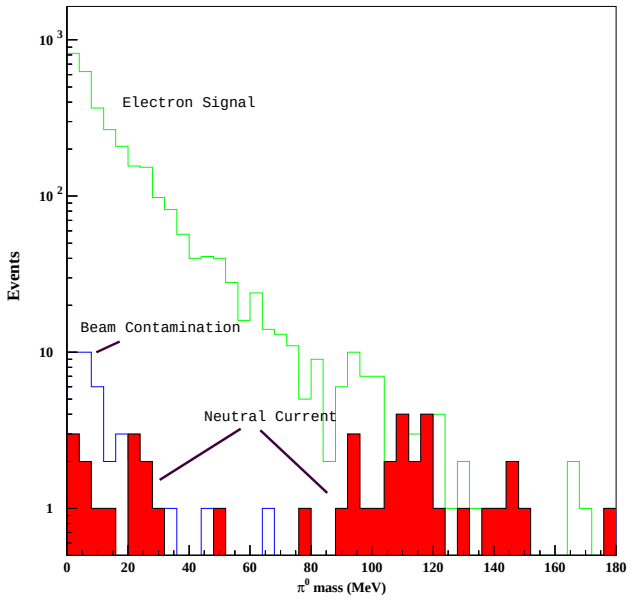

Figure 7: Rejection of π^0 background in a water Cherenkov detector. To reject π^0 in which a weak second ring was missed, each showering event with a single identified ring is analyzed to find the most likely direction and energy of an additional ring. The invariant mass formed by the second ring-candidate and the original ring tends to zero for true electrons (unfilled histograms), but is $O(m_{\pi^0})$ for many neutral-current background events. (shaded).

while the ratio between scintillation and Cherenkov light provides additional handles to separate muons from electrons.The energy range and the rejections against background needed for those experiments nicely match the requirements of our study as summarized in Table 4.

The obvious shortcut of the liquid oil technology is its relative high price compared with water. Indeed, the mass of the largest liquid oil neutrino detector (the forthcoming MiniBoone) is two orders of magnitud smaller than the mass of the largest water neutrino detector, Super-Kamiokande. One could hardly afford truly large, 50 kton or more liquid oil detectors.. Nevertheless, for the sake of a fair comparison between both technologies, in the following we will assume a detector identical to MiniBoone (449 ton of pure mineral oil, fiducial is 382 ton, with a photocathode surface coverage of 10%) but inflated to a 40 kton fiducial detector.

Neutrino-^{12}C cross sections are taken from reference[15]. They come from an upgraded version of the continuous random phase approximation method used to com-

Reaction	Suppression factor
$\nu_\mu C \to \mu^- X$	10^{-3}
$\nu_\mu C \to \nu_\mu \pi^\circ X$	10^{-2}
$\nu_\mu C \to \mu^- \pi X$	10^{-4}
$\nu_\mu C \to \nu_\mu \pi X$	10^{-3}
$\nu_\mu e \to \nu_\mu e$	10^{-1}
$\nu_e C \to e^- X$	0.5

Table 4: Background suppression and signal efficiency in the MiniBooNE detector. Numbers are quoted in the 50 MeV - 1 GeV energy range.

pute $\nu - ^{12} C$ cross-sections and in average they are lower by about $\sim 15\%$ from what quoted by the MiniBoone experiment.

Table 5 shows the background event distributions, assuming no ν_μ-$\nu_e$oscillation (e.g., driven by θ_{13}), for a 200 kton-year exposure to a π^+ and a π^- focused beams. As before, intrinsic ν_e contamination from the beam results to be the dominant background.

π^+ focused beam			π^- focused beam		
Channel	Initial sample	Final sample	Channel	Initial sample	Final sample
ν_μ^{CC}	2538	2.5	$\overline{\nu}_\mu^{CC}$	451	0.5
ν_e^{CC}	12	6	$\overline{\nu}_e^{CC}$	2.3	1.0
NC (visible)	48	0.5	NC	10	< 0.1
$\nu_\mu \to \nu_e$	100%	50%	$\overline{\nu}_\mu \to \overline{\nu}_e$	100%	50 %

Table 5: Summary of data samples in a π^+ and in a π^- focused neutrino beam. Numbers refer to a liquid scintillator detector of 40 kton located at a distance of 130 km from the source and a run of 5 years.

As one can see comparing tables 2,3 and 5, our estimations for the rates and performance of the liquid oil detector match quite well with our calculations concerning the water detector. The performance of both devices is quite similar, although the liquid scintillator is able to reject more neutral currents than the water Cherenkov (as one expects, given the extra handle provided by the scintillation light). The dominant background in both cases is the beam ν_e contamination. The conclusion is that one would probably prefer, for this experiment, a water detector, where one can afford truly gargantuan sizes.

5. Sensitivity

In this section we illustrate the sensitivity that a 40 kton water or liquid oil detector, located at 130 km from the source would have to the various parameters of

the neutrino CKM matrix.

5.1. Sensitivity to the atmospheric parameters

A 40 kton detector placed at L=130 Km has excellent opportunities of precision measurements of $\sin^2\theta_{23}$ and Δm^2_{23} with a $\nu_\mu$disappearance experiment. Given the mean beam energy of the $\nu_\mu$beam $(1.27\cdot L/E)^{-1} = 1.6\cdot 10^{-3}$ eV^2/c^4 and so $p(\nu_\mu \to \nu_\mu)$ results to be just at its minimum.

To illustrate the precision in measuring δm^2_{atm} and θ_{23} in case of positive signal Figure 8 shows the result of a 200 kton-years exposure experiment (5 years of a 40 kton detector) in case the oscillation occurs with $\sin^2(2\theta_{23})$=0.98 and $\delta m^2_{atm} = 3.8, 3.2$ or 2.5 eV^2/c^4. The computation is performed defining 4 energy bins in the 0.1-0.7 GeV energy range and including Fermi motion, that is by far the most limiting factor to energy reconstruction at these energies. See[24] for more details. We find that Δm^2_{23} can be measured with a standard deviation of $1 \cdot 10^{-4}$ eV^2/c^4 while $\sin^2 2\theta_{23}$ is measured at the 1% level.

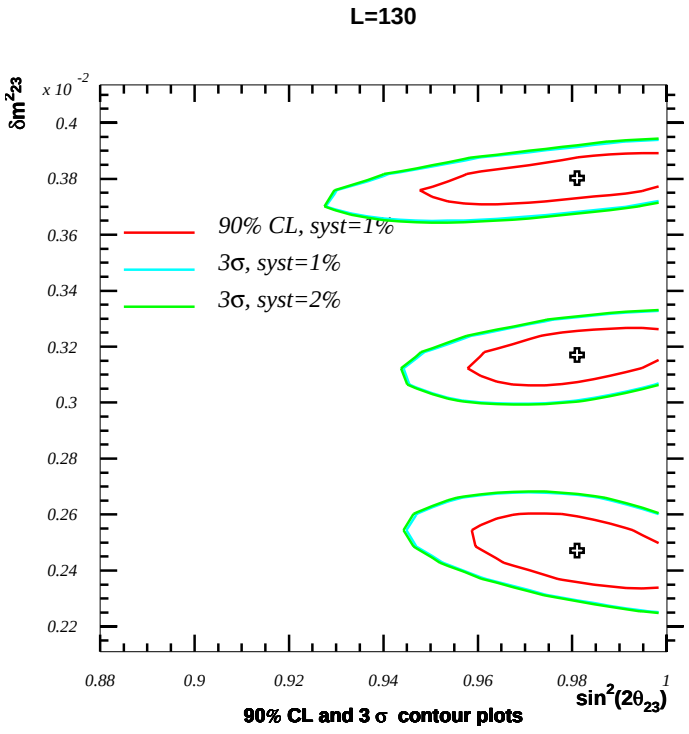

Figure 8: Fits of δm^2_{atm} (eV^2),$\sin^2(2\theta_{23})$ plane after 5 years of run, for a systematic error of 2% and a distance of 130 km. The crosses sign the initial points $(0.98, 3.8\cdot 10^{-3})$, $(0.98, 3.2\cdot 10^{-3})$, $(0.98, 2.5\cdot 10^{-3})$ in δm^2_{atm},$\sin^2(2\theta_{23})$ coordinates.

5.2. Sensitivity to θ_{13} in the SMS-MSW scenario

Here we assume, for simplicity that the solar parameters, δm_{12} and θ_{12} correspond to the small angle solution of the solar neutrino problem. In this case, the oscillation probability simplifies to:

$$P_{\nu_e\nu_\mu} = \sin^2 2\,\theta_{13}\sin^2\theta_{23}\sin^2\frac{\Delta m^2_{23}L}{4E_\nu} \tag{4}$$

that is, the oscillation depends only on the atmospheric parameters and θ_{13}. For the present study, only statistical errors are considered. Given the 2.5:1 disparity between expected beam and detector backgrounds, it is likely that beam-related uncertainties will be the most important, and these can be controlled by measuring the beam with a near detector and using data from the HARP[25] experiment to refine the hadronic production model.

As an example Figure 9 shows the expected sensitivity for a 5-year run with a 40 kton (fiducial) water target at a distance of 130 km, using a π^+ focused neutrino beam from the SPL.

5.3. Sensitivity to CP in the LMA-MSW scenario

In the remaining of this section we will assume that the solar parameter lie in the upper range of the large mixing angle solution (LMA-MSW) of the solar problem, specifically we will assume maximal mixing in the solar sector and $\delta m^2_{12} = 10^{-4}$ eV^2. We consider a water detector.

Unfortunately, the $\bar{\nu} + {}^{16}O$ cross-section is approximately six times less than that for $\nu + {}^{16}O$ at these energies, diminishing the experiment's sensitivity to CP-violation considerably (about the same considerations apply to Carbon, in the case of liquid oil detectors).

We follow the approach in[29,30] and fit simultaneously the CP phase δ and θ_{13}. Notice that, although we apply a full three family treatment to our calculations, including matter effects, these are not important at the short distances and low energies considered. Notice also that the measurement of the solar parameters will be performed by Kamland[31], well before the experiment described here, and that the determination of the atmospheric parameters, done with muon disappearance, as illustrated above, is also largely uncorrelated from the measurement of the other parameters.

Figure 10 shows the confidence level contours for a simultaneous fit of $\theta_{13}$and δ, corresponding to three values of θ_{13}, $\theta_{13} = 5^\circ, 8^\circ, 10^\circ$, and a maximally violating CP phase, $\delta = \pm 90^\circ$. The results include statistical errors as well as those due to background subtraction. Since the sensitivity is dominated by the low antineutrino

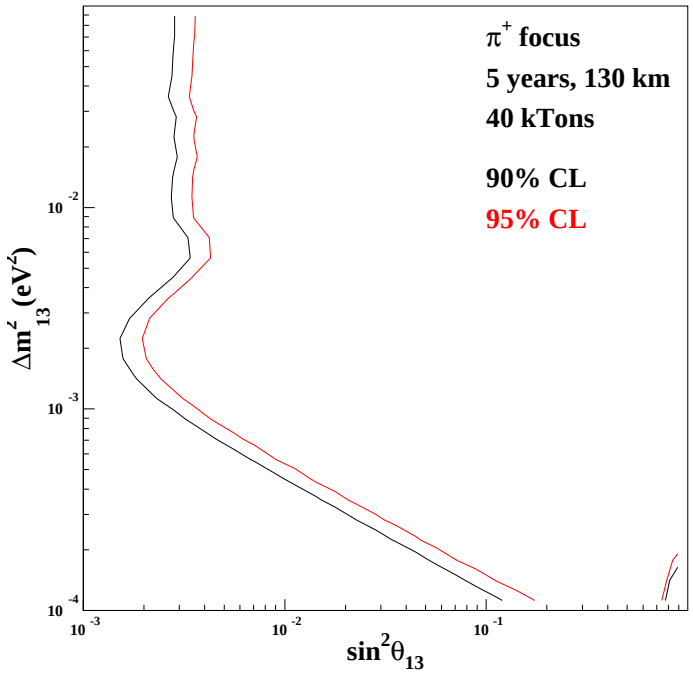

Figure 9: Oscillation sensitivity for π^+ focused neutrino beams. The outer(inner) contours are the regions where the expected confidence level to reject the oscillation hypothesis in the absence of oscillation exceeds 90%(95%).

statistics, we have considered for this exercise a 10 year run with focused π^- and a 2 year run with focused π^+.

Inspection of Figure 10 permits to draw two immediate conclusions. The first one is that the sensitivity to CP does not worsen very much when θ_{13} becomes (moderately) smaller, as pointed out in[32,29,30]. The second is that, at 90 % confidence level, a maximally violating CP phase ($\delta = \pm 90°$) would be just distinguishable from a non CP violating phase ($\delta = 0°$). Recall that this is only in the upper limit of the LMA regime. In conclusion, this experiment would offer a chance to observe CP violation if nature would conspire to offer a very lucky scenario (maximal CP violation, solar square mass difference as large as allowed by current data).

Figure 11 shows the result of the same fit, now assuming a very large water detector, such as the proposed UNO[33] water Cherenkov apparatus, with a fiducial mass of 400 ktons. Clearly, the prospects to observe CP violation are much improved.

6. Conclusions

We have examined the physics potential of a low energy super beam which could be produced by the CERN Super Proton Linac. Water Cherenkov and liquid oil

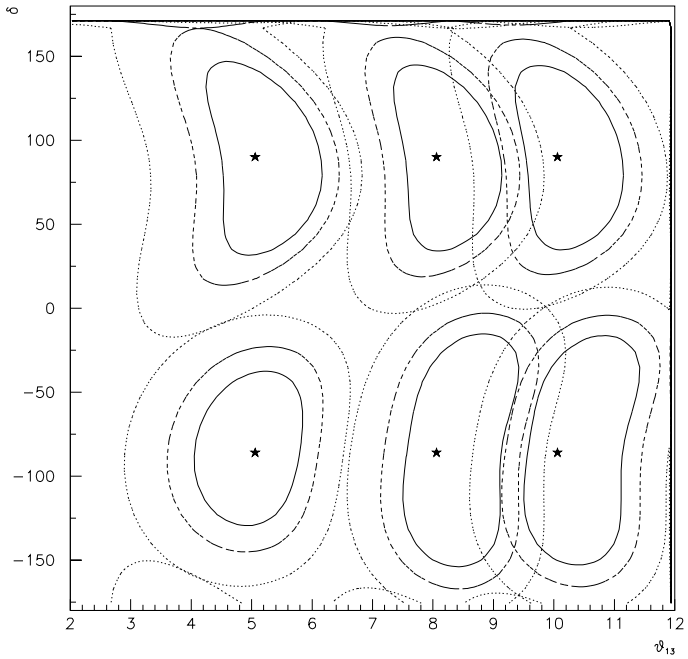

Figure 10: one sigma, 90 % and 99 % confidence level intervals resulting from a simultaneous fit to the θ_{13} and δ parameters. The generated values were $\theta_{13} = 5°, 8°, 10°$, $\delta = \pm 90°$. A full three family treatment is used. Statistical errors as well as those due to background substraction are taken into account. We have considered a 10 year antineutrino and a 2 year neutrino run, at 130 km with a 40 kton detector.

scintillator detectors have been considered. Detailed calculations have been performed for the case of the water detector.

The low energy of the beam studied has several advantages. Beam systematics is reduced with respect to high energy, since one is below kaon production. Furthermore, e/μ and e/π^0 separation in a water (liquid oil) detector is near optimal at this low energies. The drawback are the small anti neutrino cross sections, which are more than a factor five smaller than neutrino cross sections.

The peak of the oscillation is at a distance of about 100 km. An ideal location, at 130 km from CERN exists, the Modane laboratory in the Frejus tunnel.

A "moderate" size detector ("only" twice as big a Super-Kamiokande) at this baseline could, in a five year run, improve our knowledge of the atmospheric parameters by about one order of magnitude (with respect to the expected precision of next generation neutrino experiments, such as Minos). It could also measure θ_{13} if its magnitude is bigger than about 3°, again, more than one order of magnitude the precision of next generation experiments. For comparison, one could do slightly better in the neutrino factory (about a factor two to three) for what concerns the atmospheric

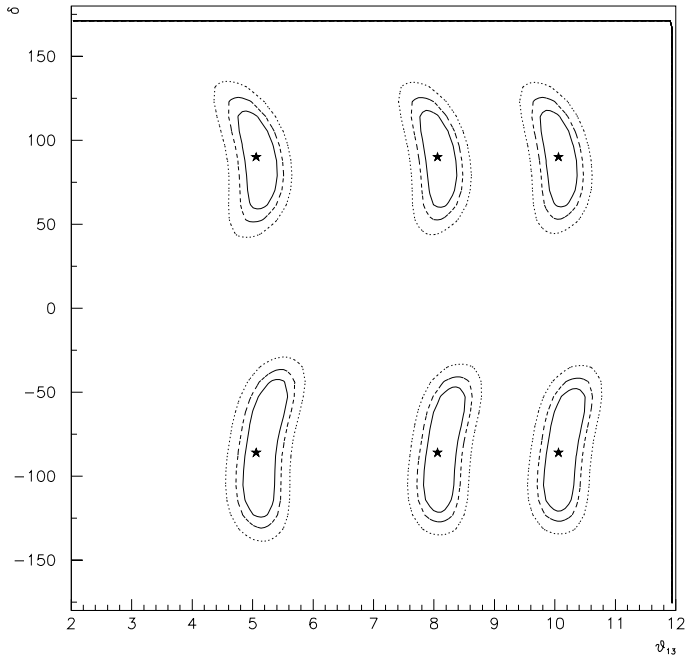

Figure 11: one sigma, 90 % and 99 % confidence level intervals resulting from a simultaneous fit to the θ_{13} and δ parameters. The generated values were $\theta_{13} = 5°, 8°, 10°$, $\delta = \pm 90°$. A full three family treatment is used. Statistical errors as well as those due to background substraction are taken into account. We have considered a 10 year antineutrino and a 2 year neutrino run, at 130 km with a 400 kton detector.

parameters, and more than one order of magnitude better for θ_{13}.

Such a detector could also, if the solution to the solar neutrino problem lies in the upper part of the LMA, distinguish, eventually, a maximally violating CP phase. Here, the performance if much worst than the one expected for the neutrino factory. For CP violation studies a very large detector, á la UNO (400 kton fiducial mass) is mandatory.

7. Acknowledgements

We wish to thank the Super-Kamiokande collaboration for allowing use of its simulation and analysis software in this study.

8. References

1) B. Richter, "Conventional Beams or Neutrino Factories: The Next Generation of Accelerator-Based Neutrino Experiments", SLAC-PUB-8587.

2) V. Barger, S. Geer, R. Raja and K. Whisnant, Phys.Rev.D63:113011,2001.
3) V. Barger et al., FERMILAB-FN-703, Mar 2001. 42pp.hep-ph/0103052
4) B. Autin et al., CERN-2000-012, Dec 2000. 89pp.
5) For a recent paper of the NOMAD collaboration, see P. Astier et al., Phys.Lett.B483:387-404,2000.
6) For a recent paper of the CHORUS collaboration see E. Eskut et al., Phys.Lett.B497:8-22,2001.
7) A. de Rújula, M. B. Gavela and P. Hernández, Nucl. Phys. **B 547** (1999) 21.
8) M. Donega, Tesi di Laurea: "Study of Neutrino Oscillations with a Low Energy Conventional Neutrino Superbeam". Universit degli Studi di Milano, on 28-03-2001. See also "Neutrino fluxes from a conventional neutrino beam using the CERN SPL",Nufact note 053/2000, November, 2000.
`http://mdonega.home.cern.ch/mdonega/lowe/homepage.html`
9) N.V. Mokhov, Fermilab-FN-628(1995).
10) R. Becker-Szendy *et al.*, Nucl. Instrum. Meth. A **324**, 363 (1993).
11) K. S. Hirata *et al.* [Kamiokande-II Collaboration], Phys. Lett. B **280**, 146 (1992).
12) Y. Fukuda *et al.* [Super-Kamiokande Collaboration], Phys. Lett. B **433**, 9 (1998) [hep-ex/9803006].
13) LSND collaboration, Phys. Rev. Lett. 81, 1774 (1998).
14) Boone proposal, May 17 1997. Available at
`http://www.neutrino.lanl.gov/BooNE/boone_proposal.ps`
15) E.Kolbe et al. Nucl.Phys A613 (1997) 382, E.Kolbe et al. Nucl.Phys A652(1999) 91.
16) Luigi Mosca, talk given in the ECFA Neutrino Oscillation Working Group, May, 10th, 2001.
`http://muonstoragerings.web.cern.ch/muonstoragerings` and
`http://mdonega.home.cern.ch/mdonega/lowe/homepage.html`
17) D. Casper, private communication.
18) Michel Spiro, talk given in the plenary session, muon days, ECFA working group, May, 12th, 2001.
`http://muonstoragerings.web.cern.ch/muonstoragerings` and
`http://mdonega.home.cern.ch/mdonega/lowe/homepage.html`
19) B. Autin *et al.*, CERN-2000-012.
20) M. Shiozawa [Super-Kamiokande Collaboration], Nucl. Instrum. Meth. A **433**, 240 (1999).
21) M. D. Messier, UMI-99-23965.
22) S. Kasuga *et al.*, Phys. Lett. B **374**, 238 (1996).
23) T. Barszczak, University of California, Irvine Ph.D thesis (to be published).
24) Mauro Mezzetto, "Neutrino Oscillations at the SPL Super Beam", Nufact note 060/2000, December, 2000.

http://mdonega.home.cern.ch/mdonega/lowe/homepage.html
25) M. G. Catanesi *et al.*, CERN-SPSC-99-35.
26) Y. Fukuda *et al.* [Super-Kamiokande Collaboration], Phys. Rev. Lett. **81**, 1562 (1998) [hep-ex/9807003].
27) W. A. Mann [Soudan-2 Collaboration], Nucl. Phys. Proc. Suppl. **91**, 134 (2000) [hep-ex/0007031].
28) M. Ambrosio *et al.* [MACRO Collaboration], Phys. Lett. B **478**, 5 (2000).
29) A. Cervera et *al.*, Nucl. Phys. **B579**, 17 (2000).
30) J. Burguet-Castell,M. B. Gavela,J. J. Gomez-Cadenas,P. Hernandez and O. Mena, hep-ph/0103258.
31) KAMLAND: A REACTOR NEUTRINO EXPERIMENT TESTING THE SOLAR NEUTRINO ANOMALY. By KamLAND Collaboration (A. Piepke for the collaboration). 2001. Nucl.Phys.Proc.Suppl.91:99-104,2001.
32) A. Romanino, Nucl.Phys.B574:675-690,2000.
33) C.K. Jung "FEASIBILITY OF A NEXT GENERATION UNDERGROUND WATER CERENKOV DETECTOR: UNO". By (SUNY, Stony Brook). SBHEP-00-1, Sep 1999. 6pp. Published in In *Stony Brook 1999, Next generation nucleon decay and neutrino detector* 29-34 e-Print Archive: hep-ex/0005046.